A novel approach to *Cestrum intermedium* (mata-boi): anatomical and physical-chemical characterization, *in vitro* biological activities, and metabolites of a Brazilian native species

**Ellis Marina Szabo[1]*, Flavia Deffert[1], Vanessa Barbosa[2], Katlin Suellen Rech[1],
Isabel Christina Mignoni Homem[1], Cristiane Bezerra da Silva[1],
Vinícius Bednarczuk de Oliveira[1], Marilis Dallarmi Miguel[1],
Obdulio Gomes Miguel[1]**

*[1]Department of Pharmacy, Federal University of Paraná (UFPR), Curitiba, Paraná, Brazil,
[2]Department of Pharmacy, Campos Gerais College, Ponta Grossa, Paraná, Brazil*

The Brazilian native species *Cestrum intermedium*, known as *mata-boi*, induces hepatotoxicity and death when ingested by cattle. While most studies on this species focus on toxicological features, our study is the first to describe the anatomy and *in vitro* biological activities of *Cestrum intermedium*. We investigated adult leaves and stems by histochemistry, described their anatomy, performed physical-chemical analysis, determined *in vitro* antioxidant and antimicrobial activities, and identified secondary metabolites. A few noteworthy anatomical features were the anomocytic stomata on the abaxial surface and the absence of trichomes, in addition to the circular shaped petiole with two projections on the adaxial surface. Histochemical analysis showed chemical markers such as alkaloids, usually reported as toxic, and terpenoids. Potassium nitrate (ATR-FTIR) and lupeol palmitate (NMR) were detected on the crude stem extract. Thermogravimetric and physical-chemical analysis provided fingerprint parameters for the species. Minimal Inhibitory Concentration (MIC) assay revealed that *Staphylococcus aureus*, *Staphylococcus epidermidis*, and *Candida albicans* were weakly inhibited by extract samples. Chloroform and ethyl acetate fractions presented high phenolic content, which resulted in *in vitro* antioxidant activity. These novel features expand the knowledge about this species, considering that previous studies mainly focused on its toxicity. Our study also provided characteristics that may help in avoiding misidentification between *Cestrum* members, especially when taxonomic keys cannot be employed, as in the absence of flowers and fruits.

Keywords: Scanning electron microscopy. Chemical markers. Secondary metabolites. Alkaloids. Terpenoids. *Staphylococcus epidermidis*.

INTRODUCTION

Mata-boi belongs to the Solanaceae, a family known for containing alkaloids — usually related to the plants' toxicity — and saponins, which are known as *Cestrum* chemical markers (Vaz, 2008; Henriques, Kerber, Moreno,

2002). Brazil hosts 28 *Cestrum* species. They reside mainly in the Atlantic forest and in the Cerrado (Soares, 2006; Kissmann, Groth, 2000; REFLORA, 2020).

Cestrum intermedium Sendtn. is one of the most important toxic plants in the southern Brazilian region. When ingested by cattle, it induces liver toxicity resulting in a 70% mortality rate (Kissmann, Groth, 2000; Furlan *et al.*, 2008; Wouters *et al.*, 2013). Brazil's cattle population, which is only surpassed by India's (USDA, 2019), reached a gross value of R$ 88,6 billion in 2019 (MAPA, 2020). Southern Brazil alone held over 25%

*Correspondence: E. M. Szabo. Departamento de Farmácia. Universidade Federal do Paraná. Av. Lothário Meissner 632, 80210-170 - Curitiba, Paraná, Brasil. Phone: +55 41 99642-7239. E-mail: ellis.szabo@gmail.com. ORCID: 0000-0002-9075-9517. Flavia Deffert – ORCID: https://orcid.org/0000-0002-2188-9967. Katlin Suellen Rech – ORCID: https://orcid.org/0000-0001-6699-2450

Ellis M. Szabo, Flavia Deffert, Vanessa Barbosa, Katlin S. Rech, Isabel C. M. Homem, Cristiane B. Silva, Vinícius B. Oliveira, Marilis D. Miguel, Obdulio G. Miguel

of the gross production value (R$) on agriculture and livestock (MAPA, 2020). The country's cattle production is mostly extensive (grass fed) (USDA, 2019; EMBRAPA, 2020), meaning the livestock grazes freely, easily coming across toxic plants. These findings indicate that this native species (Vignoli-Silva, 2009) is potentially harmful to cattle — and thus economically dangerous.

Studies on this species are scarce and mainly focused on animal impairment due to the plant's toxicity. Therefore, the objective of the present study was to perform the phytochemical characterization of *Cestrum intermedium* (Szabo *et al.*, 2014) and explore features that have not been previously studied, such as anatomy and antimicrobial and antioxidant activities.

MATERIAL AND METHODS

Plant material

Cestrum intermedium aerial parts were collected in Curitiba, Paraná, Brazil (25°26'46.3"S 49°20'50.5"W) under authorization to access genetic heritage (nº 02001.001165/2013-47) granted by the Genetic Heritage Management Council (CGen) of the Brazilian Ministry of the Environment. Plant material was identified by the taxonomist Osmar dos Santos Ribas of the Botanical Museum of Curitiba (voucher MBM384025).

Extracts

Crude leaf and stem extracts were obtained from dried plant material (60°C for 12 hours in a vacuum oven) in a Soxhlet apparatus using ethanol 96 °GL for 8 hours. Crude extracts were partitioned in a modified Soxhlet. The resulting fractions were hexane, chloroform, ethyl acetate, and residual fractions. Crude extracts and fractions were concentrated until they were solvent-free.

Metabolites identification

Nuclear magnetic resonance (NMR) was carried out using $CDCl_3$, at 294 K, on a Bruker® DPX 200 MHz NMR spectrometer at 4.7 Tesla, observing ^1H and ^{13}C at 200.12 and 50.56 MHz, respectively. The chemical shifts (ppm) were determined with respect to an internal reference (TMS: 0.00 ppm) and coupling constants (J) in Hz. Metabolites were identified by Attenuated Total Reflectance–Fourier Transform Infrared spectroscopy (ATR/FTIR) (FT-IR Bruker®).

Anatomical characterization

Fresh adult leaves and stems were placed in FAA solution (formaldehyde-acetic acid-alcohol 70%) for 24 hours and then preserved in ethanol 70% until the next procedure (Berlyn, Miksche, 1976). The paradermal and cross sections of the stems and leaves were stained with Astra blue and Safranin and analyzed by light microscopy (BX40, Olympus®).

Scanning electron microscope (SEM) (JSM 6360LV, JEOL®) ultrastructure surface analysis was performed in progressively dehydrated plant material (ethanol 70% to ethanol 100%). After reaching the critical point (liquid CO_2 supplied CPD-030, Balt-Tec® apparatus), samples were gold coated (SCD-030, Balzers® apparatus). Terminology for microscopic analysis was used according to Metcalfe and Chalk (1950).

Histochemical characterization

Histochemical analysis was carried out using FAA-fixed plant material, except for the terpenoid carbonyl compounds search, which employed fresh samples. Cross sections were cut manually and stained with reagents for the detection of specific chemical groups, according to classical chemical markers identification methods (USP, 2017; Brazil, 2019). Alkaloids were detected by Dragendorff and Bertrand's reagents, flavonoids by aluminum chloride, steroids by Liebermann-Burchard, starch by Lugol, total proteins by Coomassie bright blue, neutral polysaccharides by PAS (Periodic acid-Schiff), lignin by Phloroglucinol-HCl, lipids by Sudan III, and terpenoid carbonyl compounds by 2,4-dinitrophenylhydrazine.

Physical-chemical characterization

Thermal analysis (TA) determined humidity (%) and ash content (%) in dried plant material (Brazil, 2019).

Thermogravimetric analysis (TGA) evaluated thermal degradation of dried leaves and stems by heating 10 mg samples (10 °C.min^{-1}) from 20 to 600 °C using a Labsys Evo TGA/STA-EGA (SETARAM) instrument calibrated with Indium standard (Fusion temperature: 156.6 °C; variation of the enthalpy of fusion: 28.54 J.g^{-1}) (ASTM, 2018). TGA data were statistically analyzed using Origin 9.0.

Antimicrobial activity

Antimicrobial activity of crude leaf and stem extracts and fractions was determined using agar plate diffusion and minimum inhibitory concentration (MIC) in triplicates (adapted from Veiga *et al.*, 2019). The following assays were employed: *Staphylococcus aureus* ATCC 25923, *Escherichia coli* ATCC 25922, *Pseudomonas aeruginosa* ATCC 27853, *Staphylococcus epidermidis* ATCC 12228, *Enterococcus faecalis* ATCC 29212, and *Candida albicans* ATCC 10231. Saline suspensions of the organisms were adjusted to the McFarland standard (10^8 cells per 0.49% saline solution milliliter). Ketoconazole (50 µg disks and 50 µg.mL^{-1}) and Chloramphenicol (30 µg disks and 30 µg.mL^{-1}) were used as positive controls.

Agar plate diffusion

Bacteria were grown on Muller-Hinton agar plates (2.0 g.L^{-1} beef extract, 17.5 g.L^{-1} casein hydrolysate, 1.5 g.L^{-1} starch, 17 g.L^{-1} agar) for 24 hours at 35 °C. Yeast was grown on Sabouraud agar plates (40 g.L^{-1} glucose, 10 g.L^{-1} peptone, 15 g.L^{-1} agar) for 48 hours at 26°C. Next, saline suspensions of the organisms (10^8.mL^{-1}) were inoculated on agar plates with sample paper disks (1000 µg per disk, dried before inoculation). Bacteria inhibition halos were measured after 24 hours at 35 °C and yeast inhibition halos were measured after 48 hours at 26 °C.

Minimal inhibitory concentration (MIC)

Sample serial dilutions were evaluated in bacteria and yeast saline suspensions (10 µL of 10^8.mL^{-1} per well).

Test microplates, which were previously incubated at 35 °C for 24 hours (bacteria) and at 26 °C for 48 hours (yeast), received 20 µL of 2,3,5-triphenyltetrazolium chloride (TTC) 0.5% (*m/v*). After incubating at 35 °C for 1 hour, viable organisms developed a reddish color.

Phenol contents

The phenol content of fractions and crude leaf and stem extracts was determined in triplicates, employing the method of Singleton, Orthofer and Lamuela-Raventos (1999). The calibration curve (available on the supplementary material), which was used to interpolate samples' absorbance at 760 nm, was produced by combining gallic acid (2,5 – 20 µg.mL^{-1}) with the Folin-Ciocalteu reagent. Results were expressed as gallic acid equivalents (mg.g^{-1} GAE).

Antioxidant activity

The *in vitro* antioxidant activity of fractions and crude leaf and stem extracts was evaluated by phosphomolybdenum complex reduction and 2,2-diphenyl-1-picrylhydrazyl (DPPH) radical reduction in triplicates. Antioxidant activity data were submitted to ANOVA and Tukey test (α=0.05).

Phosphomolybdenum complex reduction

The reduction assay employed by Prieto, Pineda and Aguilar (1999) was used to compare samples to Ascorbic acid and Rutin standards. Sample activities were compared to standards at 695 nm. Results were expressed in relative antioxidant activity (RAA%).

DPPH radical reduction

The free radical scavenging assay employed by Mensor *et al.* (2001) was used to compare samples to Ascorbic acid and Rutin standards at 568 nm. Samples (5 – 50 µg.mL^{-1}) were evaluated to determine 50% of DPPH reduction (IC$_{50}$). The IC$_{50}$ was determined using a calibration curve.

Ellis M. Szabo, Flavia Deffert, Vanessa Barbosa, Katlin S. Rech, Isabel C. M. Homem, Cristiane B. Silva, Vinícius B. Oliveira, Marilis D. Miguel, Obdulio G. Miguel

RESULTS AND DISCUSSION

Anatomical characterization

Leaves presented wavy and thin cell walls (Figure 1A) and wavy epidermis (Figure 1B) covered by a striated cuticle (Figure 1C). Anomocytic stomata were observed only on the abaxial surface, which characterizes *Cestrum intermedium* leaves as hypostomatic (Figure 1D, E, and F).
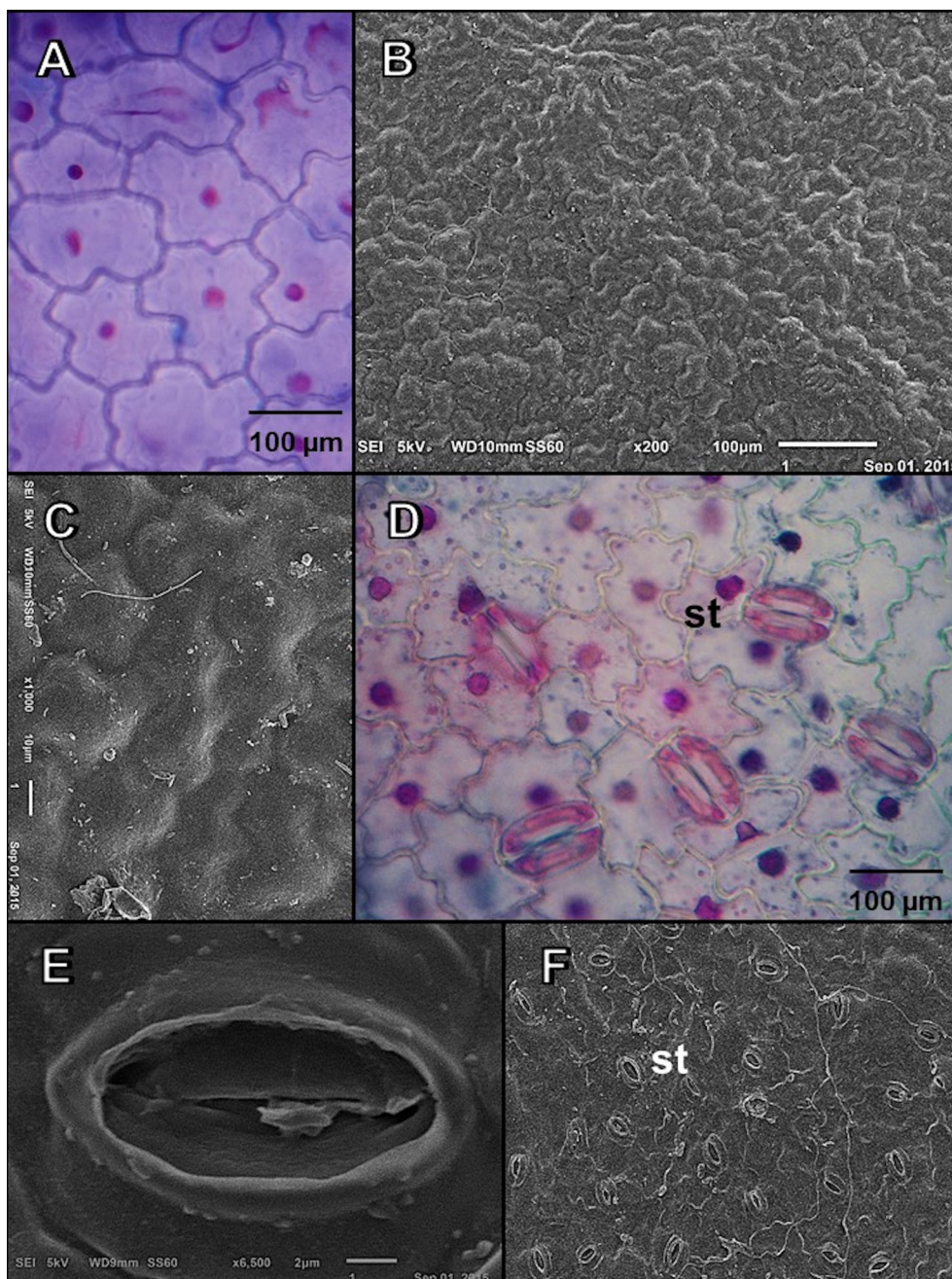
FIGURE 1 - *Cestrum intermedium (Solanaceae) – Leaf front view.*

A, B- Adaxial surface in front view. C- Epidermis detail revealing wavy and slightly striate cuticle. D- General view of stomata in abaxial surface. E- Detailed stomata. F- Abaxial surface irregular feature and stomata. **Note**: st- stomata.

Leaf cross section (Figure 2A) revealed slightly larger epidermal cells on the adaxial surface (Figure 2B, F, and G) when compared to the abaxial surface (Figure 2D); a thicker cuticle was observed on the adaxial surface (Figure 2B and F). Midrib was concave-convex (Figure 2A) and presented a C-shaped vascular bundle with a secondary xylem interspersed with phloem cells surrounded by a sheath of sclerenchyma cells (Figure 2C). Small vascular bundles (Figure 2E) were found in the dorsiventral mesophyll (Figure 2F). A single-layered palisade parenchyma was observed. The spongy parenchyma was composed of 3-4 strata (Figure 2F and G).
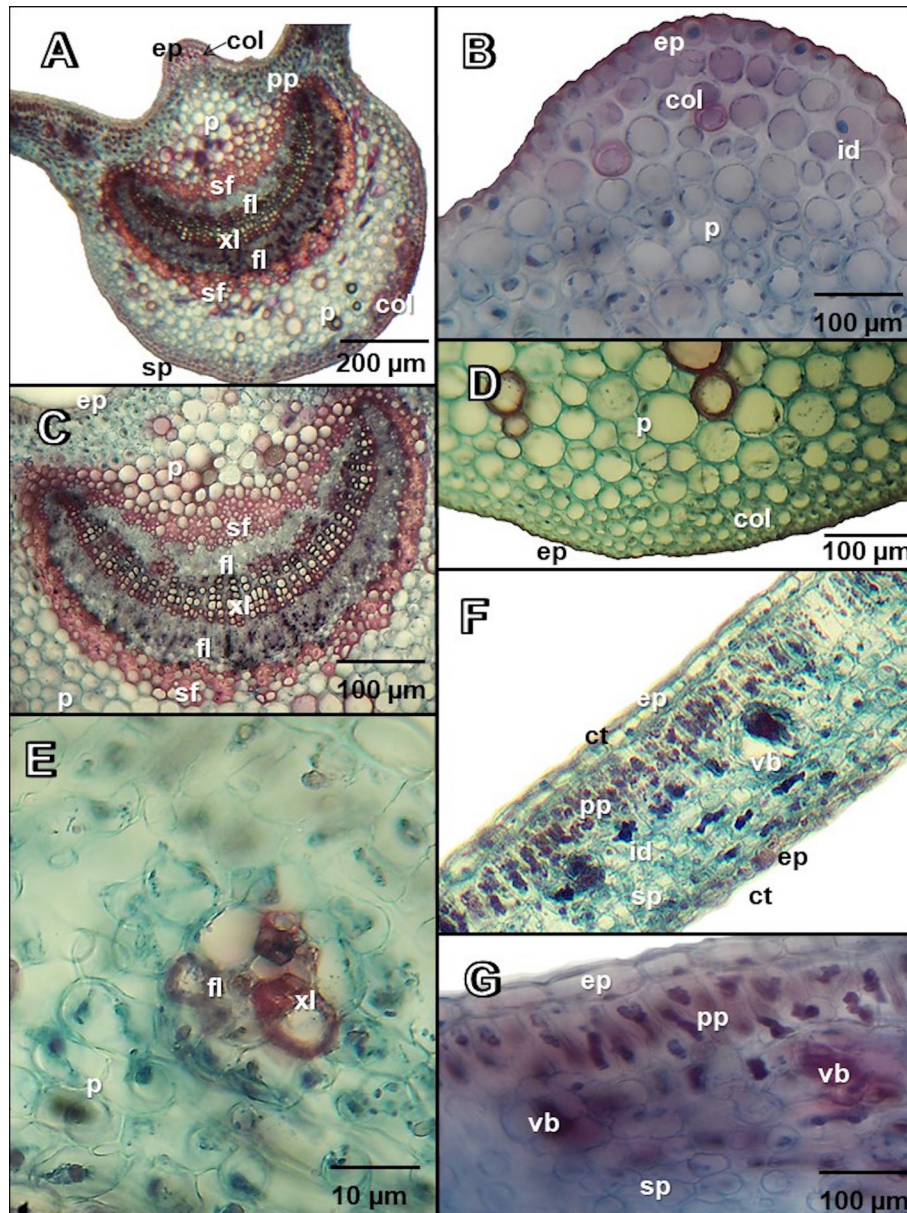
FIGURE 2 - *Cestrum intermedium (Solanaceae). Leaf – Cross Section.*

A- General aspect. B, D- Epidermis and collenchyma with idioblasts details. C- Midrib detail. E- Mesophyll detail revealing midsized vascular bundle. F- Dorsiventral mesophyll revealing palisade and spongy parenchyma with idioblasts. G- Epidermis detail. **Note:** ep- epidermis, col- collenchyma, p- parenchyma, pp- palisade parenchyma, sp- spongy parenchyma, sf- sclerenchyma fibers, id- idioblasts, ct- cuticle, xl- xylem, fl- phloem, vb- vascular bundle.

Petiole was circular shaped with two projections on the adaxial surface (Figure 3A) and presented isodiametric epidermal cells covered by a striated cuticle (Figure 3B). The uniseriate epidermis had features resembling those of the midrib (Figure 3C) and presented a thick-walled parenchyma in close-up (Figure 3D). Petiole vascular system showed an open C-shaped bicollateral vascular bundle and few sclerenchyma cells surrounding the phloem, which were more abundant in the abaxial surface (Figure 3E and F).
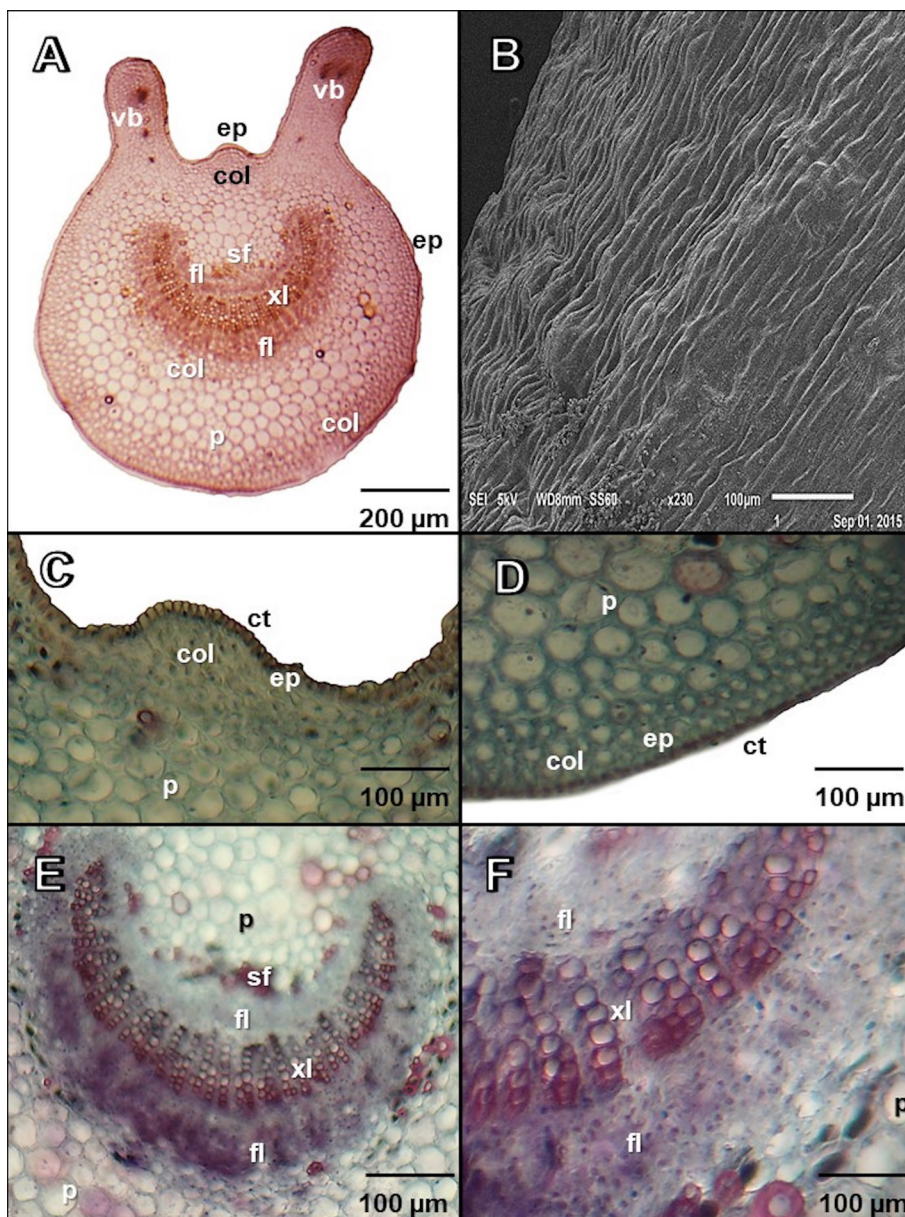
FIGURE 3 - *Cestrum intermedium (Solanaceae). Petiole.*

A- General view. B- Epidermis irregular aspect in detail. C, D- Epidermis and collenchyma details. E- Arc-shaped collateral vascular bundle detail. F- Phloem-xylem interchange in vascular bundle detail. **Note:** ep- epidermis, col- collenchyma, p- parenchyma, sf- sclerenchyma fibers, fl- phloem, ct- cuticle, xl- xylem.

The general aspect of the stems showed a circular shape in cross-section (Figure 4A) and irregular bark (Figure 4C). Surrounded by sclerenchyma cells (5-7 strata), the cortical parenchyma was juxtaposed to few angular collenchyma cells (Figure 4B). The vascular cylinder showed a wide secondary xylem placed between two phloem layers (Figure 4E): the outer phloem layer presented few parenchyma cells (Figure 4E) and the inner phloem layer was over the sclerenchyma cells, which surrounded medullary parenchyma with relatively large and slightly lignified cells (Figure 4D and E).
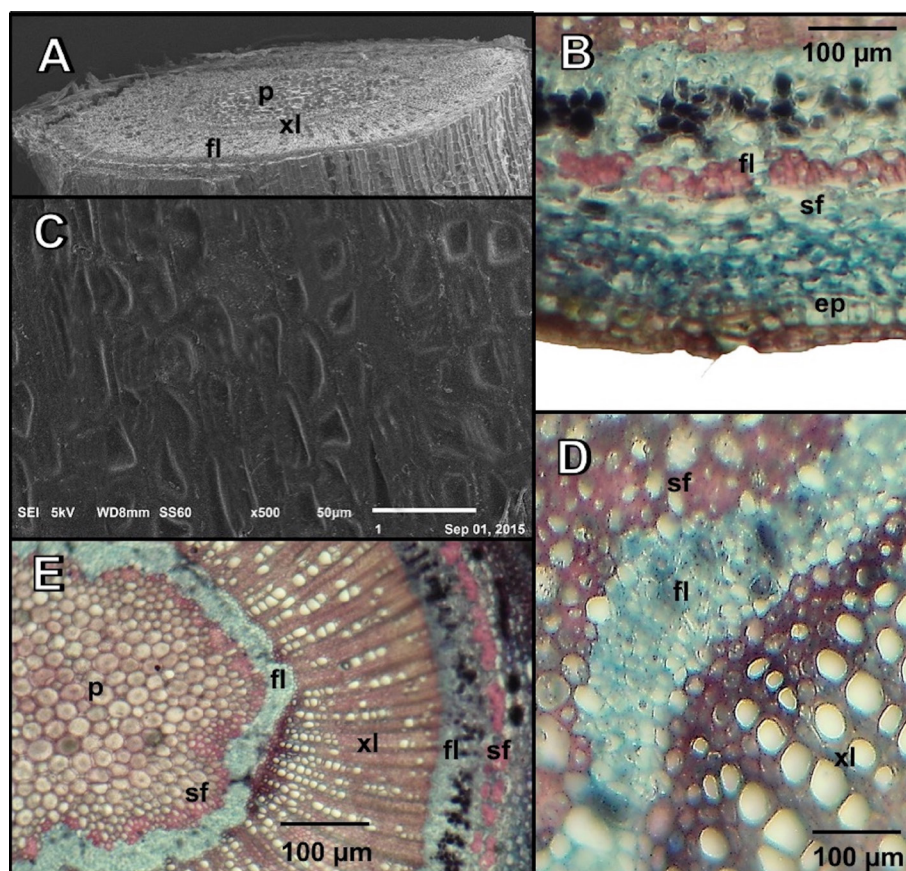
FIGURE 4 - *Cestrum intermedium (Solanaceae). Stem.*

A- Stem cross section. B- Stem detail, revealing anatomical structure. C- Irregular epidermis general view. D- Vascular bundle detail: xylem tracheids, bilateral phloem, and sclerenchyma fibers. E- Vascular bundle general view: xylem tracheids, bilateral phloem, and sclerenchyma fibers. **Note:** ep- epidermis, col- collenchyma, p- parenchyma, sf- sclerenchyma fibers, fl- phloem, xl- xylem.

Cestrum intermedium anatomy resembled that of other genus species (Gallego, 2011; Jáurequi, Benítez, 2007; Liscovsky, Cosa, 2005), especially with features such as the uniseriate epidermis and abaxial anomocytic stomata. Wavy cuticle was also observed in *C. humboldtii* (Ahmad, 1964), *C. auranticum*, and *C. diurnum* (Jáurequi; Benítez, 2007).

Important features for the differentiation of similar species, trichomes can also be applied to differentiate *Cestrum* species (Gallego, 2011): *Cestrum intermedium, C. parqui* (Soares, 2006), and *C. glabrum* are glabrous, but many species present trichomes (Gallego, 2011). For example, branched trichomes were observed in *C. diurnum* and *C. nocturnum* (Jáurequi; Benítez, 2007).

Another feature used to differentiate species is cell wall thickness on leaf epidermis. Cell walls are generally thick as observed in *C. diurnum* and *C. nocturnum*, but they are slender in *C. jaramillanum* (Jáurequi; Benítez, 2007) and *C. intermedium*. Table I compares *Cestrum intermedium* to other *Cestrum* species. Due to *Cestrum*'s complex taxonomy and interspecies distinction challenges, *Cestrum intermedium*'s detailed anatomy and histochemical features may assist in individuals' identification. This study provides a valuable strategy, since *Cestrum's* main identification strategies rely on taxonomic keys, which require the presence of flowers and fruits for adequate employment, restricting the species recognition.

TABLE I - Comparison of *Cestrum intermedium* to other *Cestrum* species

	LEAF					PETIOLE			STEM			
	Epidermis	Stomata	Cuticle	Vascular Bundle	Trichome	Epidermis	Vasc. Bundle	Trichome	Epidermis	Cuticle	Vas. Bundle	Trichome
C. intermedium	Uniseriate; Square cells; Wavy;	Anomocytic; Hypostomatic;	Slender; Striated; Thicker in adaxial surface;	C-shaped (midrib);	Absent;	Uniseriate;	C-shaped; Bicollateral;	Absent;	Uniseriate;	Striated;	Bicollateral;	Absent;
C. diurnum	Uniseriate; Elongated outer cells; Nishtha, Rao (2017) Square and rectangular; Jáuregui, Benítez (2007)	Anomocytic; Hypostomatic; Jáuregui, Benítez (2007)	Thick; Ornamented in adaxial surface; Jáuregui, Benítez (2007)	Oval open bicollateral; Nishtha, Rao (2017) Closed colateral; Jáuregui, Benítez (2007)	Glandular in abaxial surface; Jáuregui, Benítez (2007)	Uniseriate; Jáuregui, Benítez (2007)	Closed bicollateral; Jáuregui, Benítez (2007)	Scarce; Glandular; Jáuregui, Benítez (2007)	Uniseriate; Rectangular; Nishtha, Rao (2017)	-	Bicollateral; Nishtha, Rao (2017)	-
C. nocturnum	Uniseriate; Nishtha, Rao (2017) Uniseriate; Mainly rectangular; Jáuregui, Benítez (2007)	Anomocytic; amphistomatic; Jáuregui, Benítez (2007) Hypostomatic; Liscovsky and Cosa (2005)	Thick; Jáuregui, Benítez (2007) Smooth; Liscovsky and Cosa (2005)	Open plane-convex; Nishtha, Rao (2017) Closed colateral; Jáuregui, Benítez (2007)	Glandular; scarcer in adaxial surface; Jáuregui, Benítez (2007)	Uniseriate; Jáuregui, Benítez (2007)	Closed bicollateral; Jáuregui, Benítez (2007)	-	Uniseriate; Nishtha, Rao (2017)	-	Bicollateral; Nishtha, Rao (2017)	-
C. amictum	-	-	Smooth; Liscovsky and Cosa (2005)	-	Glandular; Liscovsky and Cosa (2005)	-	-	-	Uniseriate; Liscovsky and Cosa (2005)	Uniseriate; Liscovsky and Cosa (2005)	-	-
C. laevigatum	-	-	Smooth; Liscovsky and Cosa (2005)	-	Glandular; Liscovsky and Cosa (2005)	-	-	-	Uniseriate; Liscovsky and Cosa (2005)	Striated; Liscovsky and Cosa (2005)	-	-
C. parqui	-	Hypostomatic; Occasional amphistomatic; Liscovsky and Cosa (2005)	Striated; Liscovsky and Cosa (2005)	-	Glandular; Liscovsky and Cosa (2005)	-	-	-	Uniseriate; Liscovsky and Cosa (2005)	Striated; Liscovsky and Cosa (2005)	-	-
C. sendtnerianum	-	Hypostomatic; Liscovsky and Cosa (2005)	Smooth; Liscovsky and Cosa (2005)	-	-	-	-	-	Uniseriate; Liscovsky and Cosa (2005)	Smooth; Liscovsky and Cosa (2005)	-	-

Histochemical characterization

Histochemical characterization identified common chemical groups — such as proteins, polysaccharides, lignin, and lipids — and chemical markers — such as alkaloids and terpenoid carbonyl compounds. Total proteins were detected around xylem cells in leaf midrib and petiole (Figure 5A and 6A), and in stem phloem and angular parenchyma cells (Figure 7A and B). Neutral polysaccharides were observed in leaf blade epidermis and xylem (Figure 5B and C), petiole xylem (Figure 6B and C), and in stem xylem, fibers, and medullary parenchyma (Figure 7C). Lignified cells were observed in petiole xylem, fibers, and leaves and stem xylem, as expected. Stem epidermis featured a strongly lignified cuticle (Figures 5H, 6 G, 7H, and I). Lipids were present in leaves' epidermis (Figure 5I), petiole (Figure 6J), and stem endodermis (Figure 7J). Starch grains were present in leaf and petiole parenchyma (Figure 5J and 6H) and in stems medullary parenchyma (Figure 7K).

Terpenoid carbonyl compounds were identified in leaf parenchyma, fibers, and xylem (Figure 5K and L), petiole (Figure 6I and K), and in stem medullary parenchyma (Figure 7L). Reagents for alkaloids showed a positive result in leaves, petioles, and stems. Alkaloids were observed between xylem cells, sclerenchyma fibers, secondary vascular bundles, and some spongy parenchyma cells (Figure 5D, E, F, and G). Petiole presented alkaloids in parenchyma cells, sclerenchyma fibers, and some xylem areas (Figure 6D, E and F). The stem presented alkaloids in medullary parenchyma idioblasts and sclerenchyma fibers, in minor amounts (Figure 7D, E, F, and G).
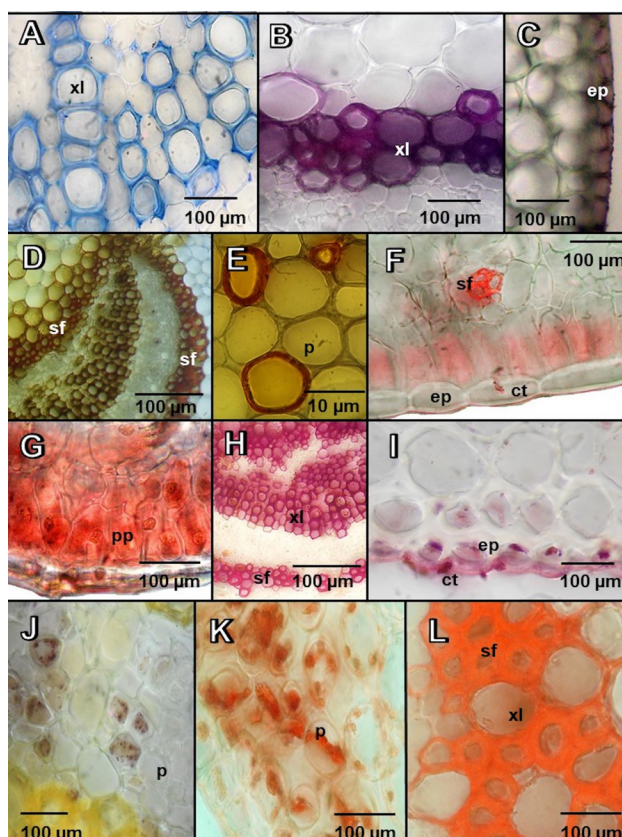
FIGURE 5 - *Cestrum intermedium (Solanaceae). Histochemical characterization- Leaf.*

A- Positive reaction for total proteins (Coomassie bright blue). B, C- Positive reaction for neutral polysaccharides (PAS – periodic acid-Schiff). D, E- Positive reaction for alkaloids (Dragendorff method). F,G- Positive reaction for alkaloids (Bertrand method). H- Positive reaction for lignin (Phloroglucinol-HCl). I- Positive reaction for lipids (SUDAN III). J- Positive reaction for starch grains (Lugol). K,L- Positive reaction for terpenoid carbonyl compounds (2,4-dinitrophenylhydrazine). **Note:** ep- epidermis, p- parenchyma, sf- sclerenchyma fibers, ct- cuticle, xl- xylem.

Ellis M. Szabo, Flavia Deffert, Vanessa Barbosa, Katlin S. Rech, Isabel C. M. Homem, Cristiane B. Silva, Vinícius B. Oliveira, Marilis D. Miguel, Obdulio G. Miguel
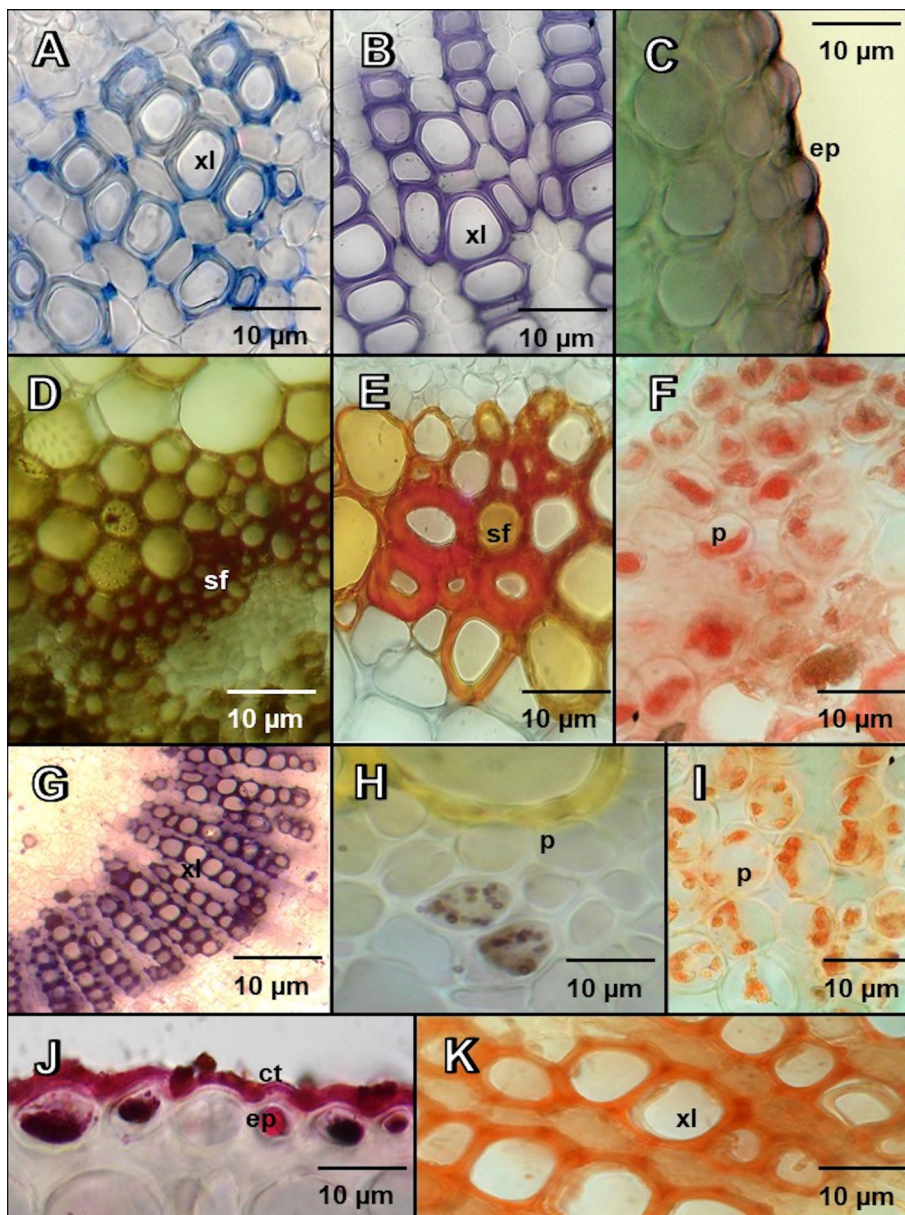
FIGURE 6 - *Cestrum intermedium (Solanaceae). Histochemical characterization- Petiole.*

A- Positive reaction for total proteins (Coomassie bright blue). B, C- Positive reaction for neutral polysaccharides (PAS – periodic acid-Schiff). D- Positive reaction for alkaloids (Dragendorff method). E, F- Positive reaction for alkaloids (Bertrand method). G- Positive reaction for lignin (Phloroglucinol-HCl). H- Positive reaction for starch grains (Lugol). I, K- Positive reaction for terpenoid carbonyl compounds (2,4-dinitrophenylhydrazine). J- Positive reaction for lipids (SUDAN III). **Note:** ep- epidermis, p- parenchyma, sf- sclerenchyma fibers, ct- cuticle, xl- xylem.
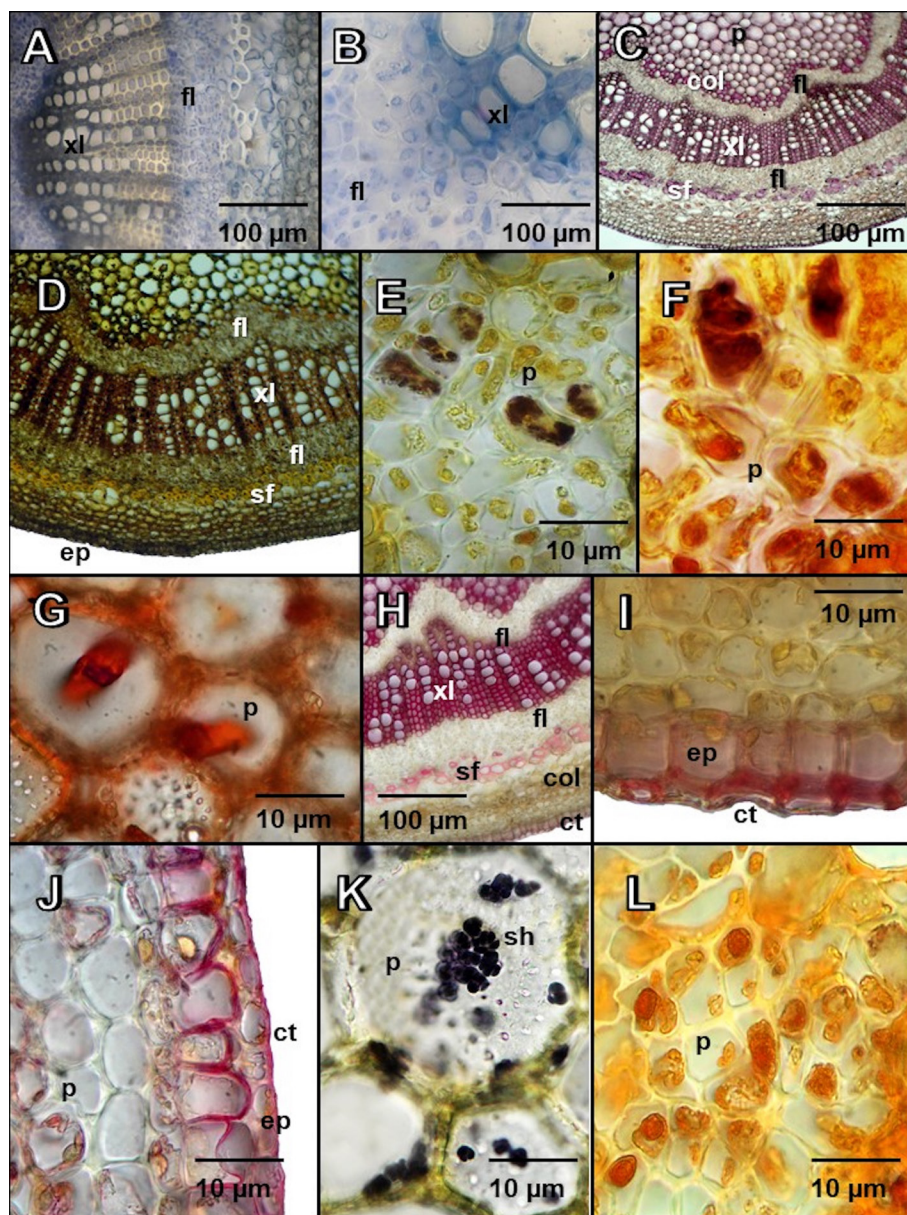
FIGURE 7 - *Cestrum intermedium (Solanaceae). Histochemical characterization - Stems.*

A, B- Positive reaction for total proteins (Coomassie bright blue). C- Positive reaction for neutral polysaccharides (PAS – periodic acid-Schiff). D, E- Positive reaction for alkaloids (Dragendorff method). F, G- Positive reaction for alkaloids (Bertrand method). H, I- Positive reaction for lignin (Phloroglucinol-HCl). J- Positive reaction for lipids (SUDAN III). K- Positive reaction for starch grains (Lugol). L- Positive reaction for terpenoid carbonyl compounds (2,4-dinitrophenylhydrazine). **Note:** ep- epidermis, p- parenchyma, fb- sclerenchyma fibers, ct- cuticle, xl- xylem, sh- starch.

The species' chemical profile was shown by histochemical analysis, which revealed alkaloids, Solanaceae chemical markers, and terpenoids. These findings were also reported on the single phytochemical screening performed in leaf and stem extracts of *Cestrum intermedium* (Szabo *et al*., 2014). Table II shows the results of the histochemical analysis, highlighting previous findings of the reported phytochemical screening.

TABLE II - Comparison of phytochemical screening results to histochemical analysis

Chemical Group	Leaves	Petiole	Stems
Total Proteins	+	+	+
Neutral Polysaccharides	+	+	+
Alkaloids	+	+	+
Lignin	+	+	+
Total Lipids	+	+	+
Starch	+	+	+
Terpenoid carbonyl compounds	+	+	+

*Shaded lines indicate groups detected in phytochemical screening by Szabo (2014).

Physical-chemical characterization

Despite indicating similar degradation temperatures, the thermogravimetric analysis (TGA) also revealed different decomposition processes, since leaves degraded in fewer stages than stems (Figure 8). TGA (Table III) showed that leaves presented thermostability up to 156 °C and stems up to 160 °C, as Stage 1 represents plant material dehydration (humidity loss). When comparing TGA to TA (Table IV), a similar humidity profile was observed. Stages 2 and 3 comprise the pyrolytic composition of woody tissues such as hemicellulose (250-300 °C), cellulose (300-350 °C), and lignin (above 400 °C), for which inert atmosphere decomposition temperatures are well established (Carrier *et al.*, 2011; Poletto *et al.*, 2010). Stage 4 (stems 1.89% mass loss) is associated with corky material, which was observed in stem histochemical analysis but was absent in leaves. The residue stage covers carbonific residue: due to the oxygen deprived atmosphere, remaining carbon residues are not combusted, which results in a stable mass. When combusted, carbonific residue becomes ash, identified by the non-volatile inorganic substances shown in Table IV.
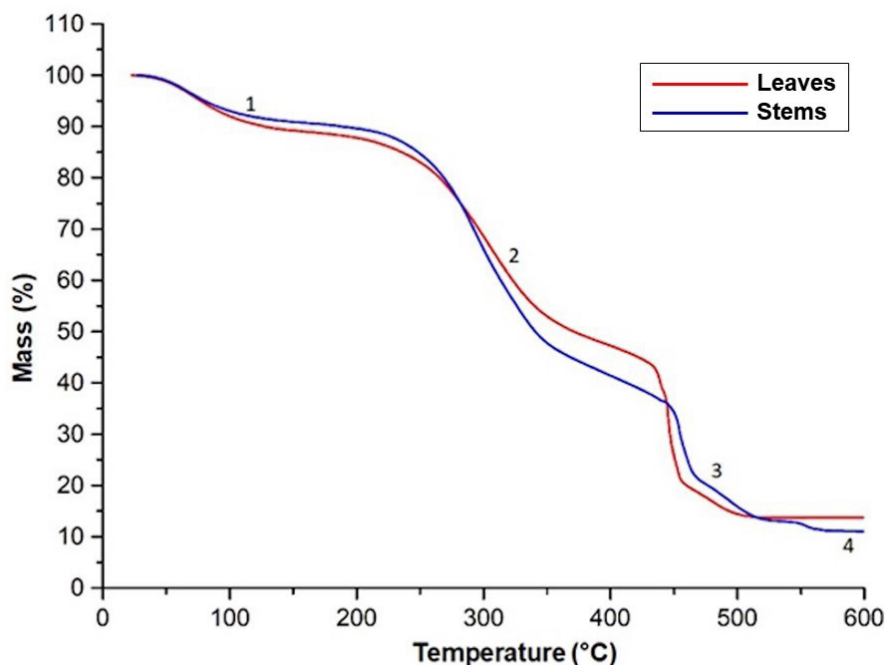
FIGURE 8 - *Graphical representation of mass decay during Thermogravimetric Analysis.*

TABLE III - Leaf and stem mass loss during TGA

Stage	Leaves				Stems			
	T (°C)		Mass Loss (%)		T (°C)		Mass Loss (%)	
1	T_I	20	10.7		T_I	20	9.29	
	T_F	156			T_F	160		
2	T_I	156	41.21		T_I	160	48.50	
	T_F	396			T_F	393		
3	T_I	396	34.14		T_I	393	29.26	
	T_F	539			T_F	535		
4	T_I	-	-		T_I	535	1.89	
	T_F	-			T_F	600		
Residue	T_I	600	13.95		T_I	600	11.06	
	T_F	-			T_F	-		

*TGA: Thermogravimetric Analysis

TABLE IV - Leaf and stem humidity and ash residue estimated by TGA and TA

Sample	Humidity%		Ash residue%
	TA	TGA	
Leaf	8.54±0.27	10.7	11.34±0.16
Stem	8.19±0.21	9.29	5.24±0.04

*TA and TGA: Thermal Analysis and Thermogravimetric Analysis

Thermogravimetric analysis showed four thermal decomposition stages with mass loss in specific temperature ranges: water evaporation; volatilization of extractives (secondary metabolites); hemicellulose decomposition; and cellulose decomposition with slower lignin decomposition in a wider temperature range (Poletto *et al.*, 2010), which can be broken down into dehydration, active pyrolysis, and passive pyrolysis (Brand *et al.*, 2018). Water loss TGA and TA profiles were similar but not identical, since the two methods have different sensitivities. Stem degradation took one additional stage due to its corky material, which takes higher temperatures to degrade.

Metabolites identification

The white amorphous powder (Compound 1), directly isolated from crude stem extract during filtration, was submitted to ATR-FTIR, since the NMR spectra presented no carbon signals. Infrared analysis revealed bands at 823 cm⁻¹, 1370 cm⁻¹, and 1767 cm⁻¹, similar to the potassium nitrate (KNO_3, 101.103 g.mol⁻¹) bands reported on the literature (Miller, Wilkins, 1952) (available on supplementary material). Potassium nitrate (Figure 9) is an inorganic salt largely used as fertilizer, food preservative, color enhancer, and dental desensitizer (PNA, 2019). Despite its broad applications, toxicological effects have been reported, especially in high concentrations: carcinogenic potential (nitrosamines), methemoglobinemia, and severe outcomes, including death (NCBI, 2020).

The yellow-white amorphous powder (Compound 2), which precipitated in crude stem extract while cooling-off, was identified as lupeol palmitate (Figure 9) ($C_{46}H_{80}O_2$, 665.1 g.mol⁻¹) by NMR, according to Liu *et al.* (1998) and Silva *et al.* (2017) (available on supplementary material). Experimental ¹H chemical shifts (δ ppm): 0.79 s, 0.84 s, 0.88 s, 0.90 s, 0.94 s, 1.03 s (H-24 – 28 and

30 – CH$_3$), 1.68 s (H-23 – CH$_3$), 4.57 s (H-29a), and 4.68 s (H-29b) — these signals are characteristic of lupeol. Experimental ^{1}H chemical shifts (δ ppm) corresponding to the palmitic fraction: 2.28 (H-2 – CH$_2$), 1.33 (H-15'), 1.1-1.4 m (H-4' to 14'). Experimental ^{13}C chemical shifts (δ ppm): 37.8 (C-1), 23.7 (C-2), 80.6 (C-3), 38.4 (C-4), 55.4 (C-5), 18.2 (C-6), 34.1 (C-7), 40.9 (C-8), 50.3 (C-9), 38.1 (C-10), 20.9 (C-11), 25.1 (C-12), 37.1 (C-13), 42.8 (C-14), 27.5 (C-15), 35.6 (C-16), 43.0 (C-17), 48.4 (C-18), 48.0 (C-19), 150.8 (C-20), 29.3 (C-21), 40.0 (C-22), 27.4 (C-23), 16.1 (C-24), 16.0 (C-25), 16.5 (C-26), 14.5 (C-27), 18.3 (C-28), 109.3 (C-29), 19.4 (C-30), 173.2 (C-1'), 34.8 (C-2'), 25.1 (C-3'), 29.7 (C-4'), 30.1 (C-13'), 31.9 (C-14'), 22.7 (C-15'), 14.5 (C-16'). In Silva *et al.* (2017), lupeol palmitate presented selective cytotoxic effects, while lupeol presented anticancer activity, protective effects for LDL oxidation, and anti-inflammatory properties (Silva *et al.*, 2017).
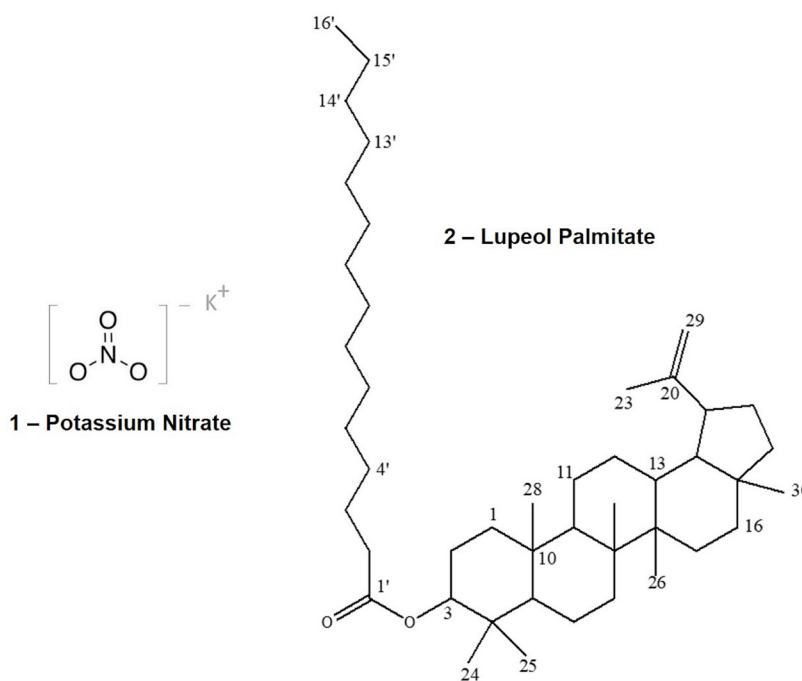
FIGURE 9 – *Molecular structures of Compound 1 and 2.*

Antimicrobial activity

Despite failing to inhibit growth in agar plates, limitations such as inadequate diffusion in agar due to lipophilic characteristics may have affected the results. Nevertheless, positive controls produced inhibition halos in cultures. Therefore, results may be considered as false-negative since MIC presented different outcomes. MIC revealed no inhibition of *Escherichia coli, Pseudomonas aeruginosa,* and *Enterococcus faecalis.* However, *Staphylococcus aureus, Staphylococcus epidermidis,* and *Candida albicans* were inhibited.

In general, plant extracts are considered active when IC$_{50}$< 100 µg.mL^{-1} (Cos *et al.*, 2006). However, inhibitory activity of plant extracts may also be classified as good (under 100 µg.mL^{-1}), moderate (100-500 µg.mL^{-1}), and weak (500-1000 µg.mL^{-1}) (Ayres *et al.*, 2008), since MIC is not determined by IC$_{50}$. *Staphylococcus epidermidis* was the most sensitive strain: the leaf presented moderate activity (hexane fraction) and weak activity (crude extract and chloroform fraction), while the stem presented weak activity (crude extract, hexane, and chloroform fractions). *Staphylococcus aureus* was weakly inhibited by most samples, except by leaf residual fraction, crude stem

extract, ethyl acetate, and residual fractions. *Candida albicans* was weakly inhibited by hexane fractions and leaf ethyl acetate fraction. Detailed outcomes are expressed in Table V.

TABLE V – Minimum Inhibitory Concentration (μg.mL^{-1}) on sensible strains

Sample	*C. albicans*	*S. aureus*	*S. epidermidis*
Crude Leaf Extract	>1000	1000	500
Leaf Hexane Fraction	1000	500	250
Leaf Chloroform Fraction	>1000	1000	500
Leaf Ethyl Acetate Fraction	1000	1000	>1000
Leaf Residual Fraction	>1000	>1000	>1000
Crude Stem Extract	>1000	>1000	1000
Stem Hexane Fraction	500	500	500
Stem Chloroform Fraction	>1000	1000	1000
Stem Ethyl Acetate Fraction	>1000	>1000	>1000
Stem Residual Fraction	>1000	>1000	>1000

Rojas *et al.* (2003) described that *Cestrum auriculatum*, despite presenting no activity against bacteria, was able to inhibit *Candida albicans* ATCC 90028, among other fungi. Bhattacharjee, Ghosh and Chandra (2005) reported the antimicrobial activity of *Cestrum diurnum*'s essential oil against *Staphylococcus aureus* and *Pseudomonas aeruginosa*. Khan *et al.* (2011) evaluated *Cestrum nocturnum*'s antimicrobial activity against *Staphylococcus aureus* ATCC 25923, *Escherichia coli* ATCC 25922, and *Pseudomonas aeruginosa* ATCC 27853, revealing inhibitory potential from 19 to 280 μg.mL^{-1} (MIC). Prasad *et al.* (2013) reported the antimicrobial activities of *Cestrum nocturnum*, *Cestrum auranticum*, and *Cestrum diurnum* against *Salmonella typhi*, *Pseudomonas aeruginosa*, *Klebsiella pneumoniae*, *Trichoderma* sp, and *Aspergillus* sp. No prior studies investigated the antimicrobial potential of *Cestrum intermedium*.

Phenol content

Hexane fractions were excluded from phenol content assay due to physical-chemical characteristics that impair absorbance readings. Leaf and stem chloroform and ethyl acetate fractions were classified (Chew *et al.*, 2011) as high in phenolic content (> 50 mg.g^{-1} GAE), especially the stem chloroform fraction (126 mg.g^{-1} GAE). Crude leaf and stem extracts and residual fractions were considered medium-high (between 30-50 mg.g^{-1} GAE) in phenolic content. Table VI presents the samples' phenol content.

TABLE VI – Crude extracts and total phenol content

Sample	mg.g^{-1} GAE**
Crude Leaf Extract	39.00
Leaf Chloroform Fraction	59.83
Leaf Ethyl Acetate Fraction	56.31
Leaf Residual Fraction	34.64
Crude Stem Extract	46.86
Stem Chloroform Fraction	126.69
Stem Ethyl Acetate Fraction	66.74
Stem Residual Fraction	36.02

* $y = 0.0392x - 0.0583$; $R^2 = 0.9964$
** Gallic Acid Equivalent

Ellis M. Szabo, Flavia Deffert, Vanessa Barbosa, Katlin S. Rech, Isabel C. M. Homem, Cristiane B. Silva, Vinícius B. Oliveira, Marilis D. Miguel, Obdulio G. Miguel

Antioxidant activity

Phosphomolybdenum complex reduction relative activity was used to compare standards to samples: considering ascorbic acid activity as 100%, rutin relative activity was nearly 45% (Table VII). The stem chloroform fraction showed the best reduction potential among samples (above 80% of Rutin's activity) as expected given its phenol content, followed by leaf chloroform fraction (nearly 60% of Rutin's activity) (Table VIII). Ascorbic acid, Rutin, stem and leaf chloroform fractions were significantly different according to the Tukey test.

TABLE VII – Crude extracts and fractions relative antioxidant activity (RAA) compared to ascorbic acid

Sample	RAA% x Ascorbic acid	Groups (Tukey Test)
Leaf Residual Fraction	7.05	a1
Leaf Hexane Fraction	9.05	a1 a2
Leaf Ethyl Acetate Fraction	10.23	a1 a2 a3
Stem Ethyl Acetate Fraction	11.33	a1 a2 a3 a4
Stem Residual Fraction	13.77	a2 a3 a4
Crude Leaf Extract	15.63	a3 a4
Crude Stem Extract	17.04	a4
Leaf Chloroform Fraction	27.19	a5
Stem Chloroform Fraction	37.39	a6
Stem Hexane Fraction	37.86	a6
Rutin	44.98	a7
Ascorbic acid	100.00	a8

*samples which belong to different groups are statistically different

TABLE VIII – Crude extracts and fractions relative antioxidant activity (RAA) compared to rutin

Sample	RAA% x Rutin	Groups (Tukey Test)
Leaf Residual Fraction	15.92	a1
Leaf Hexane Fraction	20.12	a1 a2
Leaf Ethyl Acetate Fraction	23.01	a1 a2 a3
Stem Ethyl Acetate Fraction	23.88	a1 a2 a3
Stem Residual Fraction	30.62	a2 a3 a4
Crude Leaf Extract	34.73	a3 a4
Crude Stem Extract	38.16	a4
Leaf Chloroform Fraction	60.45	a5
Stem Chloroform Fraction	82.33	a6
Stem Hexane Fraction	83.11	a6
Rutin	100.00	a7

*samples that belong to different groups are statistically different

In the DPPH radical scavenging method, an $IC_{50}>$ 500 µg.mL^{-1} is considered inactive (Mensor *et al.*, 2001). Thus, stem chloroform (187 µg.mL^{-1}) and ethyl acetate (267 µg.mL^{-1}) fractions and leaf ethyl acetate fraction (66 µg.mL^{-1}) were considered active, each belonging to different groups in the Tukey test. Ascorbic acid (6 µg.mL^{-1}) and Rutin (7 µg.mL^{-1}) had similar performances in scavenging activity and were considered statistically similar.

The diverse performances of standards suggested different antioxidant mechanisms: Rutin's reduction potential was 55% lower than Ascorbic acid, but similar in free radical scavenging. This diversity also reflected on samples, as leaf ethyl acetate scavenging capacity overcame that of samples with higher phenol content and superior performance on reduction activity.

CONCLUSIONS

Since previous studies were limited to cattle poisoning, this study contributed to enrich *Cestrum intermedium*'s knowledge by focusing on other features such as anatomical characteristics, chemical profile, and *in vitro* biological activities. This study carried out the first anatomical characterization of this species. We were able to distinguish *Cestrum intermedium* from other *Cestrum* species through parameters such as the absence of trichomes and C-shaped vascular bundles. The results of the histochemical analysis can also contribute to the toxicological discussion and research on cattle poisoning. Our analysis indicated the presence of alkaloids, terpenoids, and other chemical groups. Nevertheless, toxic chemical components remain unknown and the species chemical profile still needs to be fully established. *In vitro* biological activity assays revealed weak antimicrobial activity on the tested strains and different mechanisms of antioxidant activity, which showed that the biological activities of *Cestrum intermedium* are not limited to toxicity. We also identified the presence of lupeol palmitate (terpene) in the crude stem extract.

Due to the absence of similar studies, no available data on *Cestrum intermedium* could be found for comparison purposes. Although complementary studies are required to deepen the discussion on the potential biological activities of this species, our study was able to establish parameters for *Cestrum intermedium*. The preliminary data indicated that forthcoming studies may take on broader perspectives that go beyond toxicity and expand the knowledge on Brazilian biodiversity by investigating this native plant, which has a considerable impact on economic activities.

DISCLOSURE OF ANY CONFLICT OF INTERESTS

None.

REFERENCES

Ahmad KJ. Cuticular studies with special reference to abnormal stomatal cells in Cestrum. J Indian Bot Soc. 1964;43(1):165-177.

American Society for Testing and Materials (ASTM). ASTM E1363-18: Standard Test Method for Temperature Calibration of Thermomechanical Analyzers. 2018.

Ayres MCC, Brandão MS, Vieira-Junior GM, Menor JCAS, Silva HB, Soares MJS, Chaves MH. Antibacterial activity of useful plants and Chemical constituents of the roots of Copernecia prunifera. Braz J Pharmacog. 2008;18(1):90-97. Available at: https://doi.org/10.1590/S0102-695X2008000100017

Berlyn GP, Miksche JP. Botanical microtechnique and cytochemistry. Ames: Iowa State University, 1976.

Bhattacharjee I, Ghosh A, Chandra G. Antimicrobial activity of the essential oil of Cestrum diurnum (L.) (Solanales: Solanaceae). Afr J Biotechnol. 2005;4(4):371-374.

Brand MA, Barnasky RRS, Carvalho CA, Buss R, Waltrick DB, Jacinto RC. Thermogravimetric analysis for characterization of the pellets produced with different forest and agricultural residues. Cien Rural. 2018;48(11):01-10.

Brazil. Agência Brasileira de Vigilância Sanitária (ANVISA). Métodos de Farmacognosia. Farmacopeia Brasileira. Brasília: 6 ed., ANVISA, 2019, p. 311 – 340.

Brazil. Empresa Brasileira de Pesquisa Agropecuária (EMBRAPA). Qualidade da carne: do campo à mesa. Brasília: EMBRAPA, 2020.

Brazil. Ministério da Agricultura, Pecuária e Abastecimento (MAPA). Valor da Produção Agropecuária de 2019 atinge recorde de R$ 630,9 bilhões. 2020. Retrieved from: https://www.gov.br/agricultura/pt-br/assuntos/noticias/valor-da-producao-agropecuaria-encerra-2019-com-r-630-9-bilhoes. Access in:11/08/2020.

Carrier M, Loppinet-Serani A, Denux D, Lasnier JM, Ham-Pichavant F, Cansell F, et al. Thermogravimetric analysis as a new method to determine the lignocellulosic composition of biomass. Biomass Bioenergy. 2011;35(1):298-307.

Chew YL, Chan EW, Tan PL, Lim YY, Goh JK. Assessment of phytochemical content, polyphenolic composition, antioxidant and antibacterial activities of Leguminosae medicinal plants in Peninsular Malaysia. BMC Complementary Altern Med. 2011;11(12):1-10.

Cos P, Vlietink AJ, Berghe DV, Maes L. Anti-infective potential of natural products: how to develop a stronger in vitro 'proof-of-concept'. J Ethnopharmacol. 2006;106(3):290-302.

Furlan FH, Luciolli J, Borelli V, Faria Junior O, Rabelatto SV, Gava A, et al. Intoxicação por Cestrum intermedium (Solanaceae) em bovinos no Estado de Santa Catarina. Acta Sci Vet. 2008;36(3):281-284.

Gallego DC. Cestrum de Colombia (Solanaceae): estudio taxonómico de las especies de tricomas simples. [Master's dissertation] Bogota: Universidad Nacional de Colombia, 2011.

Henriques AT, Kerber VA, Moreno PRH. Farmacognosia: da planta ao medicamento. Florianópolis/Porto Alegre: UFSC e UFRGS, 2002.

Jáuregui D, Benítez CE. Anatomía foliar de siete especies de Cestrum L. (Solanaceae) y clave para especies de Venezuela. Acta Cient Venez. 2007;58(3-4):75-83.

Khan MA, Inayat H, Khan H, Saeed M, Khan I, Rahman I. Antimicrobial activities of the whole plant of Cestrum nocturnum against pathogenic microorganisms. Afr J Biotechnol. 2011;5(6):612-616.

Kissmann KG, Groth D. Plantas infestantes e nocivas. 2 ed. São Paulo: BASF, 2000.

Liscovsky IJ, Cosa MT. Anatomia comparativa de hoja y tallo em los representantes de Cestreae G. Don (Solanaceae) de Argentina. Gayana Bot. 2005;62(1):33-43.

Liu XK, LI XR, Qiu MH, Nie RL. Triterpene Constituents from Balanophora indica. Acta Bot Yuannanica. 1998;20(3):369-373.

Mensor LL, Menezes FS, Leitão GG, Reis AS, Santos TC, Coube CS, et al. Screening of brazilian plant extracts for antioxidant activity by the use of DPPH free radical method. Phytother Res. 2001;15(2):127-130.

Metcalfe CR, Chalk L. Anatomy of the dicotyledons. Oxford: Clarendon Press, 1, 1950.

Miller FA, Wilkins CH. Infrared Spectra and Characteristic Frequencies of Inorganic Ions. An Chem. 1952;24(8):1253-1294.

National Center for Biotechnology Information (NCBI). PubChem Database. Potassium nitrate, CID=24434. 2020. Retrieved from https://pubchem.ncbi.nlm.nih.gov/compound/24434. Access in: 11/08/2020.

Nishtha R, Rao A. Phytochemical analysis and anatomical study of two species of Cestrum from Chandigarh. Int J Pharm Sci Res. 2017;8(12):5234-5240.

Poletto M, Dettenborn J, Pistor V, Zeni M, Zattera AJ. Materials produced from plant biomass. Part I: evaluation of thermal stability and pyrolysis of wood. Mater Res. 2010;13(3):375-379.

Prasad MP, Prabhu A, Thakur MS, Yogesh RM. Phytochemical screening, antioxidant potential and antimicrobial activities in three species of cestrum plants. Int J Pharmacol Biol Sci. 2013;4(2):(B)673-678.

Prieto P, Pineda M, Aguilar M. Spectrophotometric quantitation of antioxidant capacity through the formation of a Phosphomolybdenum Complex: specific application to the determination of vitamin E. Anal Biochem. 1999;269(2):337-341.

A novel approach to *Cestrum intermedium* (mata-boi): anatomical and physical-chemical characterization, *in vitro* biological activities, and metabolites of a Brazilian native species

---

Potassium Nitrate Association (PNA). About potassium nitrate. 2019. Retrieved from http://www.kno3.org.

REFLORA. Cestrum L. accepted names in Brazil. Available at: <http://floradobrasil.jbrj.gov.br/reflora/listaBrasil/Consulta PublicaUC/BemVindoConsultaPublicaConsultar.do?invalidate PageControlCounter=1&idsFilhosAlgas=%5B2%5D& idsFilhosFungos=%5B1%2C10%2C11%5D&lingua=en &grupo=5&familia=null&genero=cestrum&especie =&autor=&nomeVernaculo=&nomeCompleto=&forma Vida=null&substrato=null&ocorreBrasil=SIM& ocorrencia=OCORRE&endemismo=TODOS&origem= TODOS&regiao=QUALQUER&estado=QUALQUER& ilhaOceanica=32767&domFitogeograficos=QUALQUER& bacia=QUALQUER&vegetacao=TODOS&mostrarAte= SUBESP_VAR&opcoesBusca=NOME_ACEITO&login Usuario=Visitante&senhaUsuario=&contexto=consulta-publica>. Access in: 11/08/2020.

Rojas R, Bustamante B, Bauer J, Fernández I, Albán J, Lock O. Antimicrobial activity of selected Peruvian medicinal plants. J Ethnopharmacol. 2003;88(2-3):199-204.

Silva ATM, Magalhães CG, Duarte LP, Mussel WN, Ruiz ALTG, Shiozawa L, et al. Lupeol and its esters: NMR, powder XRD data and in vitro evaluation of cancer cell growth. Braz J Pharm Sci. 2017;53(3):1-10.

Singleton VL, Orthofer R, Lamuela-Raventos RM. Analysis of total phenols and other oxidation substrates and antioxidants by means of Folin–Ciocalteu reagent. Methods Enzymol. 1999;29:152-178.

Soares ELC. Estudos taxonômicos em Solanaceae lenhosas no Rio Grande do Sul, Brasil. [Master's dissertation] Porto Alegre: UFRGS, 2006.

Szabo EM, Homem ICM, Miguel MD, Miguel OG. Determinação de parâmetros físico-químicos e ensaio sistemático fitoquímico preliminar de Cestrum intermedium Sendtn. (Solanaceae). Visao Acad. 2014;15(4):5-16.

United States Department of Agriculture (USDA). Foreign Agricultural Service. Livestock and Poultry: World Markets and Trade. Washington, DC: 2019.

United States Pharmacopeial Convention (USP). <561> Articles of Botanical Origin, USP 40 - NF 35, p. 426-440. Rockville: United States Pharmacopeial Convention. 2017.

Vaz NP. Alcalóides Esteroidais dos Frutos Maduros de Solanum caavurana Vell. [Masters' in Chemistry dissertation] Curitiba: UFPR. 2008.

Veiga A, Toledo MGT, Rossa LS, Mengarda M, Stofella NCF, Oliveira LJ, et al. Colorimetric Microdillution Assay: Validation of a Standard Method for Determination of MIC, IC50 and IC90 of antimicrobial compounds. J Microbiol Methods. 2019;162:50-61.

Vignoli-Silva M. O Gênero Cestrum L. (Solanaceae) no Brasil extra-amazônico. [thesis] Porto Alegre: UFRGS, 2009.

Wouters ATB, Boabaid FM, Watanabe TTN, Bandarra PM, Correa GLF, Wouters F, et al. Intoxicação espontânea por Cestrum intermedium em bovinos no Sudoeste do Estado do Paraná. Pesq Vet Bras. 2013; 33(1):47-51.